



Article

# Novel Silver Complexes Based on Phosphanes and Ester Derivatives of Bis(pyrazol-1-yl)acetate Ligands Targeting TrxR: New Promising Chemotherapeutic Tools Relevant to SCLC Management

Maura Pellei <sup>1</sup>, Carlo Santini <sup>1,\*</sup>, Luca Bagnarelli <sup>1</sup>, Miriam Caviglia <sup>1</sup>, Paolo Sgarbossa <sup>2</sup>, Michele De Franco <sup>3</sup>, Mirella Zancato <sup>3</sup>, Cristina Marzano <sup>3,\*</sup> and Valentina Gandin <sup>3</sup>

<sup>1</sup> School of Science and Technology, Chemistry Division, University of Camerino, Via S. Agostino 1, 62032 Camerino, Italy

<sup>2</sup> Department of Industrial Engineering, University of Padova, Via Marzolo 9, 35131 Padova, Italy

<sup>3</sup> Department of Pharmaceutical and Pharmacological Sciences, University of Padova, Via Marzolo 5, 35131 Padova, Italy

\* Correspondence: carlo.santini@unicam.it (C.S.); cristina.marzano@unipd.it (C.M.)

**Abstract:** Bis(pyrazol-1-yl)acetic acid (HC(pz)<sub>2</sub>COOH) and bis(3,5-dimethyl-pyrazol-1-yl)acetic acid (HC(pz<sup>Me2</sup>)<sub>2</sub>COOH) were converted into the methyl ester derivatives **1** (L<sup>OMe</sup>) and **2** (L<sup>2OMe</sup>), respectively, and were used for the preparation of silver(I) complexes **3–5**. The Ag(I) complexes were prepared by the reaction of AgNO<sub>3</sub> and 1,3,5-triaza-7-phosphaadamantane (PTA) or triphenylphosphine (PPh<sub>3</sub>) with L<sup>OMe</sup> and L<sup>2OMe</sup> in methanol solution. All Ag(I) complexes showed a significant in vitro antitumor activity, proving to be more effective than the reference drug cisplatin in the in-house human cancer cell line panel containing examples of different solid tumors. Compounds were particularly effective against the highly aggressive and intrinsically resistant human small-cell lung carcinoma (SCLC) cells, either in 2D and 3D cancer cell models. Mechanistic studies revealed their ability to accumulate into cancer cells and to selectively target Thioredoxin (TrxR), thus leading to redox homeostasis unbalance and ultimately inducing cancer cell death through apoptosis.

**Keywords:** silver; bis(pyrazoly)acetate ligands; anticancer activity; TrxR; oxidative stress



**Citation:** Pellei, M.; Santini, C.; Bagnarelli, L.; Caviglia, M.; Sgarbossa, P.; De Franco, M.; Zancato, M.; Marzano, C.; Gandin, V. Novel Silver Complexes Based on Phosphanes and Ester Derivatives of Bis(pyrazol-1-yl)acetate Ligands Targeting TrxR: New Promising Chemotherapeutic Tools Relevant to SCLC Management. *Int. J. Mol. Sci.* **2023**, *24*, 4091. <https://doi.org/10.3390/ijms24044091>

Academic Editor: Geoffrey Brown

Received: 24 January 2023

Revised: 6 February 2023

Accepted: 13 February 2023

Published: 17 February 2023



**Copyright:** © 2023 by the authors. Licensee MDPI, Basel, Switzerland. This article is an open access article distributed under the terms and conditions of the Creative Commons Attribution (CC BY) license (<https://creativecommons.org/licenses/by/4.0/>).

## 1. Introduction

Medicinal inorganic chemistry offers possibilities for the design of therapeutic agents not readily available to organic compounds [1,2]. The wide range of coordination numbers and geometries, accessible redox states, thermodynamic and kinetic characteristics, and the intrinsic properties of the cationic metal ion and ligand itself offer to the medicinal chemist a wide spectrum of reactivities that can be exploited [3]. Group 11 metal complexes showed encouraging perspectives in this regard, and several Cu(I), Cu(II), Au(I), Au(III) and Ag(I) complexes were investigated for their antitumoral properties [4–8]. In particular, silver(I) coordination compounds have been recognized as promising therapeutics [9] due to their outstanding antibacterial, antimycotic, antiparasitic, antimalarial and anticancer activities [4,10,11]. Silver(I) complexes for therapeutic purposes have been prepared with a vast variety of ligands, but those scoring the best results usually contain N-heterocycles, N-heterocyclic carbenes (NHC), and phosphanes [4,12–17]. Silver(I) coordination compounds are effective against various bacteria, fungi, protozoa, and several cancer cell lines, evidencing in the latter case anticancer mechanisms that share the same biological pathways as the antibacterial ones and for these reasons are completely different from those at the basis of cisplatin cytotoxicity [18,19]. To date and to the best of our knowledge, only a few studies have been reported on the effects of silver(I) complexes on tumor xenograft murine models,

resulting in decreased growth of the tumor mass or in cell death [20–22]. Ag(I) compounds containing NHC ligands are the most promising in this respect [13,23,24].

The cytotoxic mechanisms of silver ions are based on a series of damages caused by  $\text{Ag}^+$  to the bacterial or cancer cells [4]. Nevertheless, nearly nothing is known about possible side effects that could develop after human administration of Ag(I) complexes, although silver is still considered to be nontoxic for humans and other mammals.

The efficacy of silver(I) complexes against bacteria and cancer cells depends on a number of factors: lipophilicity, redox proclivity, water solubility and stability, and rate of release of the silver ions [25]. These factors are strictly controlled by the characteristics of the ligands and their requirements in both steric and electronic properties.

In this context, bis(azol-1-yl)acetate heteroscorpionate ligands, of the general formula  $[\text{HC}(\text{CO}_2\text{H})(\text{az})_2]$  (az = N-heterocyclic ring) [26–28], have recently attracted considerable attention, and their coordination chemistry toward main group and transition metals has been extensively studied [29,30]. Among them, complexes containing bis(pyrazol-1-yl)carboxylic acids are especially of interest, due to their  $\kappa^3\text{-N,N,O}$  tripodal coordination behavior, as metalloenzyme models relevant for biochemistry [31–35] and as starting materials to yield bifunctional ligands [36–40].

We have recently reported that Cu(I) and Cu(II) complexes with heteroscorpionate ligands, obtained by conjugation of bis(pyrazolyl)acetates with nitroimidazole, glucosamine, a non-competitive NMDA receptor antagonist and the antineoplastic drug lonidamine showed cytotoxic activity toward a panel of several human tumor cell lines [36–39,41]. We have also investigated the capability of ester derivatives (methyl, isopropyl and hexyl) of bis(pyrazolyl)acetates species to form copper complexes, with in vitro antitumor activity [42], that are useful as efficient catalysts for allylic oxidations and organic macro(molecules) synthesis [43–45].

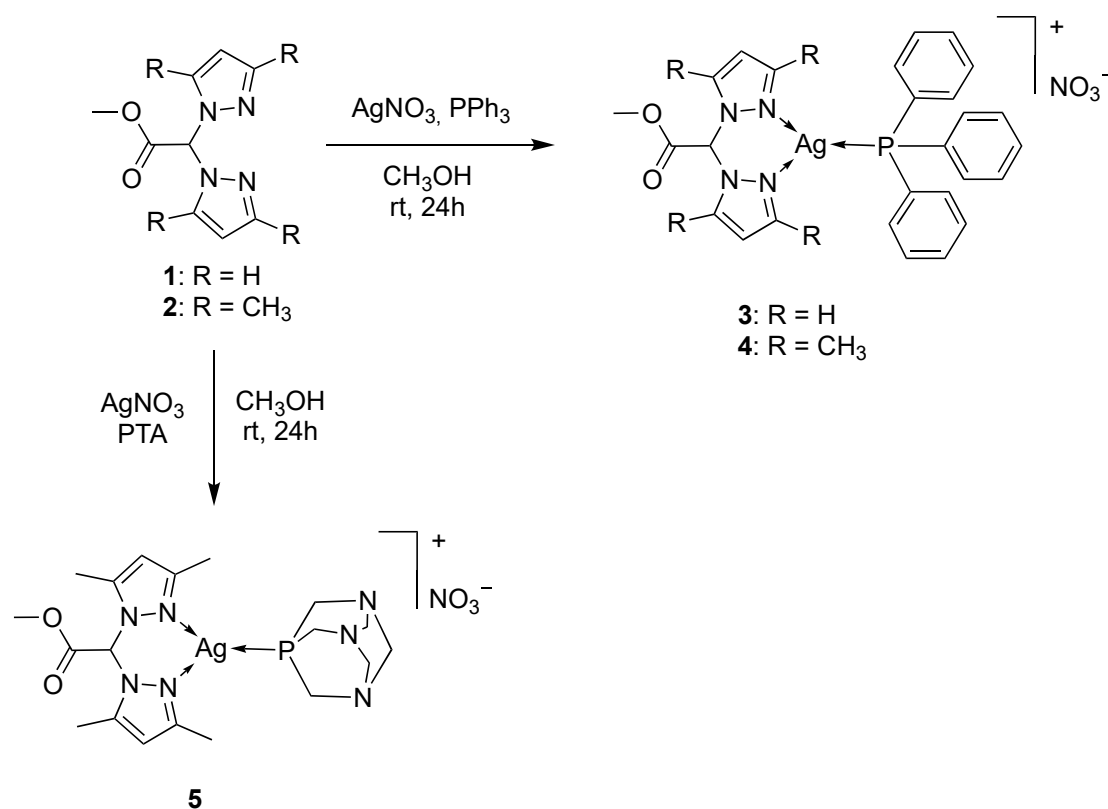
Therefore, the aim of this work was to study the capability of smaller ester derivatives of bis(pyrazolyl)acetates species to form Ag(I) complexes potentially useful for anticancer purposes. Bis(pyrazol-1-yl)acetic acid and bis(3,5-dimethyl-pyrazol-1-yl)acetic acid were converted into the methyl ester derivatives **1** ( $\text{L}^{\text{OMe}}$ ) and **2** ( $\text{L}^{2\text{OMe}}$ ) of bis(pyrazol-1-yl)- and bis(3,5-dimethyl-pyrazol-1-yl)-acetic acid, respectively, and used for the preparation of the Ag(I) complexes **3–5**. The lipophilic  $\text{PPh}_3$  and the hydrophilic PTA, able to stabilize silver in +1 oxidation state, were selected as coligands to confer different solubility properties to the resulting complexes. The new Ag(I) complexes **3–5** and the corresponding uncoordinated ligands (**1** and **2**) were investigated for their cytotoxic activity on a panel of human cancer cell lines, derived from different solid tumors, by means of both 2D and 3D cell viability studies. Mechanistic studies were performed with the aim to elucidate the molecular determinants accounting for their in vitro anticancer activity and to shed light onto the cell death mechanism triggered in SCLC cells, which were proven to be highly sensitive to their cytotoxic effects.

## 2. Results and Discussion

### 2.1. Synthesis and Characterization

The ligands  $[\text{HC}(\text{pz})_2\text{COOCH}_3]$  ( $\text{L}^{\text{OMe}}$ , **1**) and  $[\text{HC}(\text{pz}^{\text{Me}_2})_2\text{COOCH}_3]$  ( $\text{L}^{2\text{OMe}}$ , **2**) were prepared by a method described in the literature and were fully characterized.

The Ag(I) complexes  $[\text{Ag}(\text{PPh}_3)(\text{L}^{\text{OMe}})]\text{NO}_3$  (**3**) and  $[\text{Ag}(\text{PPh}_3)(\text{L}^{2\text{OMe}})]\text{NO}_3$  (**4**) were prepared from the reaction of  $\text{PPh}_3$ ,  $\text{AgNO}_3$  and the ligand  $\text{L}^{\text{OMe}}$  and  $\text{L}^{2\text{OMe}}$ , respectively, following a one-pot synthesis in methanol as solvent. Analogously, the Ag(I) complex  $[\text{Ag}(\text{PTA})(\text{L}^{2\text{OMe}})]\text{NO}_3$  (**5**) was prepared from the reaction of PTA,  $\text{AgNO}_3$  and the related ligand  $\text{L}^{2\text{OMe}}$  (Scheme 1). Attempts to synthesize the analogous compound using as starting materials  $\text{AgNO}_3$ , PTA and  $\text{L}^{\text{OMe}}$  were unsuccessful, also using different solvents and different stoichiometric ratios between the reagents.



**Scheme 1.** Chemical structures of complexes 3–5.

All the compounds are soluble in CH<sub>3</sub>OH, CH<sub>3</sub>CN and dimethyl sulfoxide (DMSO); complexes 3 and 4 are also soluble in CHCl<sub>3</sub>. The conductivity measurements for complexes 3–5, containing weakly coordinated NO<sub>3</sub><sup>−</sup> anion, are in accordance with the ionic formulations [46,47]. In particular, the molar conductance  $\Lambda_0$  for compounds 3 and 4 recorded in CH<sub>3</sub>CN is in the range 134–135  $\Omega^{-1} \text{ cm}^2 \text{ mol}^{-1}$ , in accordance with the presence of 1:1 electrolytes. The same behavior is observed for compound 5, with a  $\Lambda_0 = 25 \Omega^{-1} \text{ cm}^2 \text{ mol}^{-1}$  in DMSO solvent at 293 K. The IR spectra carried out on solid samples of the Ag(I) complexes showed all the expected bands for the chelating ligand and the phosphane coligand. The absorptions due to the C=O stretching of the ester groups are at 1760  $\text{cm}^{-1}$  and they do not significantly vary with respect to the free ligands. In the region 2849–3137  $\text{cm}^{-1}$ , the complexes exhibit weak bands typical of C-H stretchings, while the NO<sub>3</sub> vibrations appear as strong bands in the 1264–1380  $\text{cm}^{-1}$  region. In the far-IR spectra, a number of weak to medium bands in the region 200–300  $\text{cm}^{-1}$  absent in the spectra of the free ligands and of the AgNO<sub>3</sub> can be assigned to Ag–N and Ag–P vibrations, in accordance with previous assignments [48]. The <sup>1</sup>H-NMR spectra of the Ag(I) complexes, recorded in CD<sub>3</sub>CN solution at room temperature, showed a single set of resonances for the pyrazole rings, indicating that the pyrazole protons are equivalent, with a slight shift due to the coordination to the metal center. The PPh<sub>3</sub> and PTA coligands showed a characteristic series of peaks at  $\delta$  7.46–7.60 and 4.35–4.67 ppm, respectively, with an integration that confirms the 1:1 stoichiometric ratio between the ligand and the phosphane coligand. The room temperature <sup>31</sup>P{H}-NMR spectra of the Ag(I) complexes, recorded in CD<sub>3</sub>CN solution at room temperature, gave signals downfield shifted with respect to the value of the free phosphanes PPh<sub>3</sub> and PTA ( $\delta = -4.85$  and  $-102.07$  ppm, respectively). In particular, the room temperature spectrum of 3 in CD<sub>3</sub>CN gave a broad singlet centered at  $\delta$  10.67, while 4 exhibits a broad doublet with a <sup>1</sup>J(Ag-<sup>31</sup>P) coupling constant of 626 Hz. At 243 K, the spectra of 3 and 4 (in CD<sub>3</sub>CN solvent) show two doublets in which the coupling of <sup>31</sup>P to the <sup>107</sup>Ag and <sup>109</sup>Ag are resolved, in accordance with a stopped or slow phosphane exchange process. The <sup>1</sup>J(<sup>107</sup>Ag-<sup>31</sup>P) and <sup>1</sup>J(<sup>109</sup>Ag-<sup>31</sup>P) coupling constants are respectively in the range 611–624

and 705–721 Hz for compounds **3** and **4**, being of the same order of magnitude of those reported for analogous silver(I) monophosphane species [48–50]. The room temperature spectrum of **5** in CD<sub>3</sub>CN gave a broad singlet centered at  $\delta$  –84.87, while at 243 K (in CD<sub>3</sub>CN solvent), it exhibits two doublets revealing the coupling of the two silver isotopes ( $^1J(^{107}\text{Ag}-^{31}\text{P}) = 614$  Hz and  $^1J(^{109}\text{Ag}-^{31}\text{P}) = 694$  Hz), in the same order of magnitude of analogous silver(I) monophosphane species. The ratio of  $^1J(^{109}\text{Ag}-^{31}\text{P})/^1J(^{107}\text{Ag}-^{31}\text{P})$  is in good agreement with the  $^{107}\text{Ag}/^{109}\text{Ag}$  gyromagnetic ratio of 1.15.

The ESI-MS studies, performed by dissolving the Ag(I) complexes in CH<sub>3</sub>CN and recording the spectra in positive- and negative-ion mode, confirmed the formation of the PPh<sub>3</sub> and PTA complexes and the presence of nitrates as counterions. In particular, the formation of complexes **3–5** was confirmed by the presence in the positive-ion ESI-MS spectra of the major peaks attributable to the  $[\text{Ag}(\text{PPh}_3)(\text{L}^{\text{OMe}})]^+$ ,  $[\text{Ag}(\text{PPh}_3)(\text{L}^{2\text{OMe}})]^+$  and  $[\text{Ag}(\text{PTA})(\text{L}^{2\text{OMe}})]^+$  species, respectively. In the negative-ion spectra,  $[\text{Ag}(\text{NO}_3)_2]^-$  was observed as the major peak for all the complexes. The elemental analyses confirmed the stoichiometry and the purity of the products.

## 2.2. Cytotoxicity Studies

The Ag(I) complexes **3–5** and the corresponding uncoordinated ligands **1** and **2** were evaluated for their cytotoxic activity against various human cancer cell lines representative of different solid tumors. In particular, the in-house cancer cell panel contained examples of human colon (HCT-15), pancreatic (PSN-1), cervical (A431), breast (MDA-MB-231) and ovarian (2008) carcinoma as well as of SCLC (U1285). The cytotoxicity parameters, expressed in terms of IC<sub>50</sub> obtained after 72 h of exposure to the MTT assay, are reported in Table 1. For comparison purposes, the cytotoxicity of the reference metal-based chemotherapeutic drug cisplatin was assessed under the same experimental conditions.

**Table 1.** Cytotoxicity of ligands **1** and **2**, coligands PPh<sub>3</sub> and PTA, newly developed silver(I) complexes **3–5** and cisplatin on 2D cell cultures.

	IC <sub>50</sub> (μM) ± S.D.							
	HCT-15	PSN-1	A431	U1285	MDA-MB-231	2008	C13* (R.F.)	HEK293
<b>1</b>	>50	>50	>50	>50	>50	>50	>50	>50
<b>2</b>	>50	>50	>50	>50	>50	>50	>50	>50
<b>3</b>	6.5 ± 0.5	24.6 ± 0.9	4.8 ± 1.8	2.1 ± 0.3	5.4 ± 0.9	6.9 ± 1.2	5.7 ± 0.2 (0.8)	17.5 ± 1.3
<b>4</b>	9.2 ± 2.9	1.2 ± 0.4	0.9 ± 0.2	0.7 ± 0.1	10.6 ± 1.9	1.3 ± 0.2	0.20 ± 0.02 (0.2)	15.7 ± 1.8
<b>5</b>	7.4 ± 0.9	3.7 ± 0.4	1.4 ± 0.4	1.2 ± 0.2	2.8 ± 0.4	1.4 ± 0.3	0.5 ± 0.1 (0.4)	13.8 ± 2.1
<b>PPh<sub>3</sub></b>	>50	>50	47.5 ± 1.1	>50	>50	>50	>50	>100
<b>PTA</b>	>100	>100	>100	>100	>100	>100	>100	>100
<b>cisplatin</b>	15.3 ± 2.6	18.3 ± 3.1	2.1 ± 0.9	9.6 ± 1.2	30.5 ± 2.6	2.2 ± 1.0	30.5 ± 2.6 (13.9)	21.6 ± 3.5

Cells ( $3 - 8 \times 10^3 \times \text{mL}^{-1}$ ) were treated for 72 h with increasing concentrations of tested compounds. Cytotoxicity was assessed by MTT test. The IC<sub>50</sub> values were calculated by the four-parameter logistic model ( $p < 0.05$ ). R.F. = IC<sub>50</sub> (resistant subline)/IC<sub>50</sub> (wild-type cells). S.D. is standard deviation.

The three Ag(I) complexes demonstrated a marked cytotoxic activity against all tested cell lines, showing IC<sub>50</sub> values in the low/sub micromolar range, and being on average more effective than cisplatin. In particular, complexes bearing the L<sup>2OMe</sup> ligand (**4** and **5**) were the most effective derivatives, with average IC<sub>50</sub> values of 4.0 and 3.0 μM, respectively. Conversely, the L<sup>OMe</sup>-bearing derivative **3** was the weakest of the series in decreasing

cancer cell viability (average  $IC_{50}$  value of 7.5  $\mu M$ ), although it retained a cytotoxicity profile better than that of cisplatin against HCT-115, MDA-MB-231 and U1285 cancer cell lines. Bidimensional in vitro cytotoxicity screening highlighted human SCLC cells as the most sensitive to the cytotoxic effect induced by newly developed Ag(I) complexes. Actually, complexes 3–5 were from 5 up to 14 times more effective than cisplatin in decreasing U1285 cancer cell viability.

The antiproliferative activity of the Ag(I) complexes 3–5 was also investigated in an additional cell line selected for its resistance to cisplatin, the human ovarian adenocarcinoma C13\* cells. These cells were suitably selected after a cisplatin chronic treatment and are characterized by several mechanisms accounting for their resistance to cisplatin; these include (i) a reduced intracellular drug accumulation [51], (ii) high cellular levels of glutathione and metallothioneins [52], (iii) the enhanced repair of platinum-DNA adducts [53], and (iv) an overexpression of the Trx system [54].

Cytotoxicity was assessed after 72 h of drug treatment by MTT test, and the  $IC_{50}$  and RF values (RF = resistance factor, defined as the ratio of the  $IC_{50}$  of resistant cells over the  $IC_{50}$  of sensitive ones) are reported in Table 1. All new Ag(I) complexes exhibited a similar cytotoxic potency both on sensitive and resistant cells, thus proving to be capable of overcoming cisplatin resistance. Again, complexes 4 and 5 bearing the  $L^{2OMe}$  ligand were the most active compounds, being able to elicit  $IC_{50}$  values in the sub-micromolar range.

One of the main drawbacks of chemotherapeutic drugs is the possible toxic effect toward non-cancerous cells, and we measured the cytotoxicity of Ag(I) complexes against non-cancerous HEK293 cells (see Table 1). For all Ag(I) complexes, calculated  $IC_{50}$  values were higher than those obtained on average against tumor cells, thus indicating for this class of metal complexes a slightly preferential cytotoxicity against human cancer cells. In particular, the selectivity index values (SI = the quotient of the average  $IC_{50}$  toward normal cells divided by the average  $IC_{50}$  for the malignant cells) of 3–5 were 2.3, 3.9 and 4.6, respectively.

The in vitro antitumor activity of the newly developed Ag(I) derivatives was also assayed in 3D cell culture models of SCLC cells. Even if the 2D cell cultures are the most employed assays for in vitro screening due to the low cost, simplicity and reliability, two-dimensional methods are unable to reproduce the properties of in vivo solid tumors. In contrast, 3D cell cultures are much more efficient in closely mimicking the heterogeneity and complexity of the tumor mass and therefore are more predictive for in vivo results than conventional 2D cell cultures [55]. On these bases, we tested the activity of the Ag(I) complexes on spheroids obtained from U1285 cells, which were proven to be highly sensitive to their in vitro antitumor activity. SCLC spheroids were treated with the investigated compounds for 72 h, and cell viability was assessed by means of the acid phosphatase (APH) assay.

Results reported in Table 2 clearly attest that all three Ag(I) complexes were more effective than the reference drug cisplatin against 3D spheroids, being again compound 4 and 5 bearing the  $L^{2OMe}$  ligand as the most active ones. In particular, compounds 4 and 5 showed  $IC_{50}$  values averagely 2.5 times lower than that calculated for 3 and cisplatin.

**Table 2.** Cytotoxicity of ligands 1 and 2, Ag(I) complexes 3–5 and cisplatin toward U1285 cancer cell spheroids.

	$IC_{50}$ ( $\mu M$ ) $\pm$ S.D.
1	>100
2	>100
3	63.8 $\pm$ 4.4
4	27.9 $\pm$ 1.8
5	22.0 $\pm$ 2.1
cisplatin	65.4 $\pm$ 1.4



Spheroids from U1285 cells ( $3 \times 10^3$  cells/well) were treated for 72 h with increasing concentrations of tested compounds. The growth inhibitory effect was evaluated by means of the APH assay.  $IC_{50}$  values were calculated from the dose–survival curves by the four-parameter logistic model ( $p < 0.05$ ). S.D. = standard deviation.

Altogether, 2D and 3D cytotoxicity results suggested that the  $L^{2OMe}$ -bearing Ag(I) complexes were much more effective in entering cancer cells or in penetrating across the entire spheroid domain.

### 2.3. Cellular Uptake and Mechanistic Studies

To demonstrate the soundness of the above-reported supposition, we investigated the ability of tested complexes to accumulate into human U1285 cancer cells. Cells were treated for 24 h with equimolar concentrations of 3–5 ( $2 \mu\text{M}$ ), and silver content was quantified using graphite furnace atomic absorption spectrometry (GF-AAS) analysis. The results, expressed as ppm of metal per  $10^6$  cells and depicted in Figure 1, clearly confirm that the most effective derivatives 4 and 5 were those that were more effectively accumulated into human lung cancer cells. However, no linear correlation between antiproliferative activity and cellular uptake as well as between cellular uptake and logP values of the phosphane ligand could be clearly shown (see Figure S1), thus corroborating the hypothesis that lipophilicity of phosphane coligand only marginally contributes to the Ag(I) complexes uptake and efficacy profiles. On the contrary, the lipophilicity of the bidentate bis(pyrazol-1-yl)acetate ligands seems to highly contribute to their in vitro biological features, being the complexes bearing the more lipophilic  $L^{2OMe}$  ligand much more effective than those bearing the  $L^{OMe}$  one.

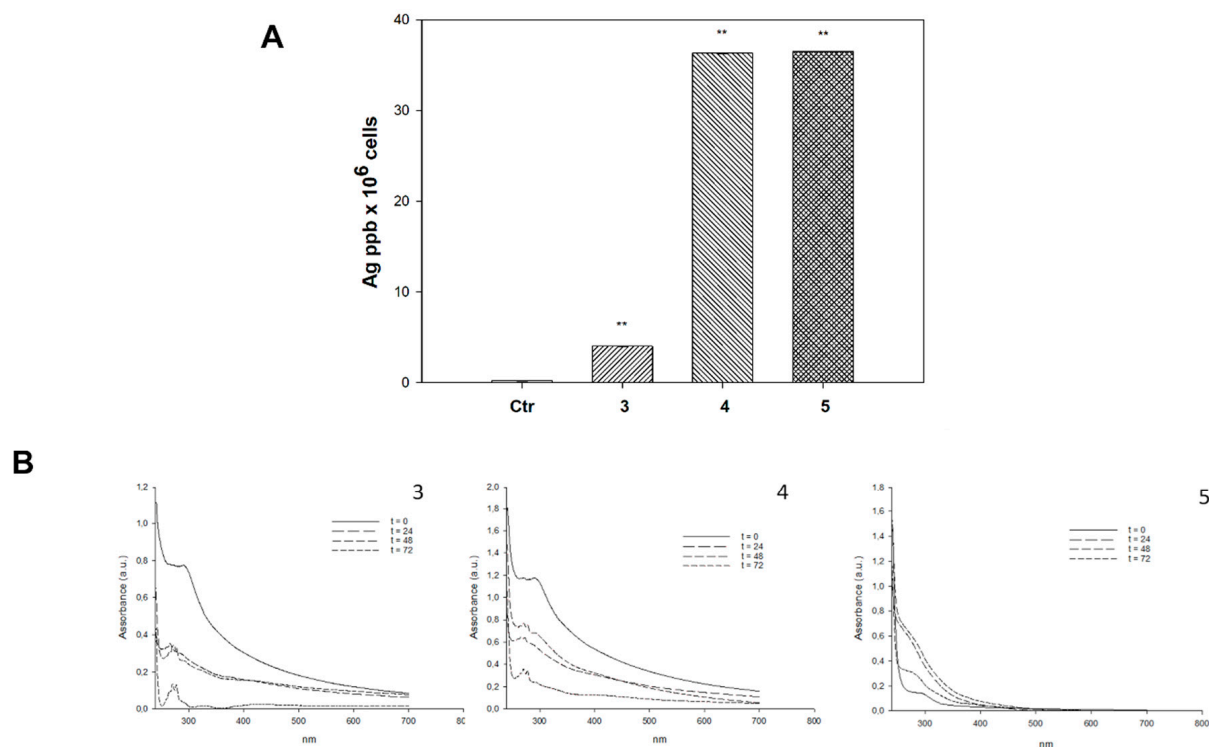


**Figure 1.** Cellular uptake and stability studies. **(A)** Intracellular accumulation of silver(I) complexes 3–5. U1285 cells were incubated with  $2 \mu\text{M}$  of silver(I) complexes for 24 h, and cellular silver content was detected by GF-AAS analysis. Error bars indicate the standard deviation. \*\*  $p < 0.01$  compared with control. **(B)** Stability studies. All complexes were dissolved at  $50 \mu\text{M}$  in 0.5% DMSO/RPMI. UV-visible spectra were recorded at  $t = 0$  min,  $t = 24$  h,  $t = 48$  h and  $t = 72$  h.

Additionally, stability studies performed in 0.5% DMSO/RPMI cell culture medium using UV–vis spectroscopy showed that complexes bearing the PPh<sub>3</sub> ligand were endowed with a scarce stability profile. Actually, significant changes were observed in the UV–vis spectra of Ag(I) complexes. This feature does not seem to affect their biological activity. Our results showing that under physiological conditions Ag(I), complex spectra rapidly (within 24 h) changed, presumably attesting the quick formation of the metal species responsible for the antiproliferative activity.

Ag(I) complexes have been widely described to be effective inhibitors of redox-active Sec-containing Thioredoxin reductase [56–58]. In addition, SCLC is endowed with elevated TrxR/Trx levels, which are known to account for radio- and chemo-resistance [59,60].

On these bases, we thought it of interest to evaluate the ability of compounds 3–5 to inhibit TrxR1 both in cell-free systems and in intact human U1285 cancer cells, and their activity was compared to that of auranofin, a well-known metal-based inhibitor of TrxR. Enzyme activity was measured according to standard procedures described in the Experimental Section, and results are shown in Figure 2A,B. In cell-free experiments, all three complexes proved to be strongly effective in inhibiting cytosolic mammalian TrxR1 in a dose-dependent manner (Figure 2A), showing IC<sub>50</sub> values in the nanomolar range (Figure 2A, insert a). However, their efficacy in *in vitro* experiments was lower than that shown by the reference TrxR inhibitor auranofin.

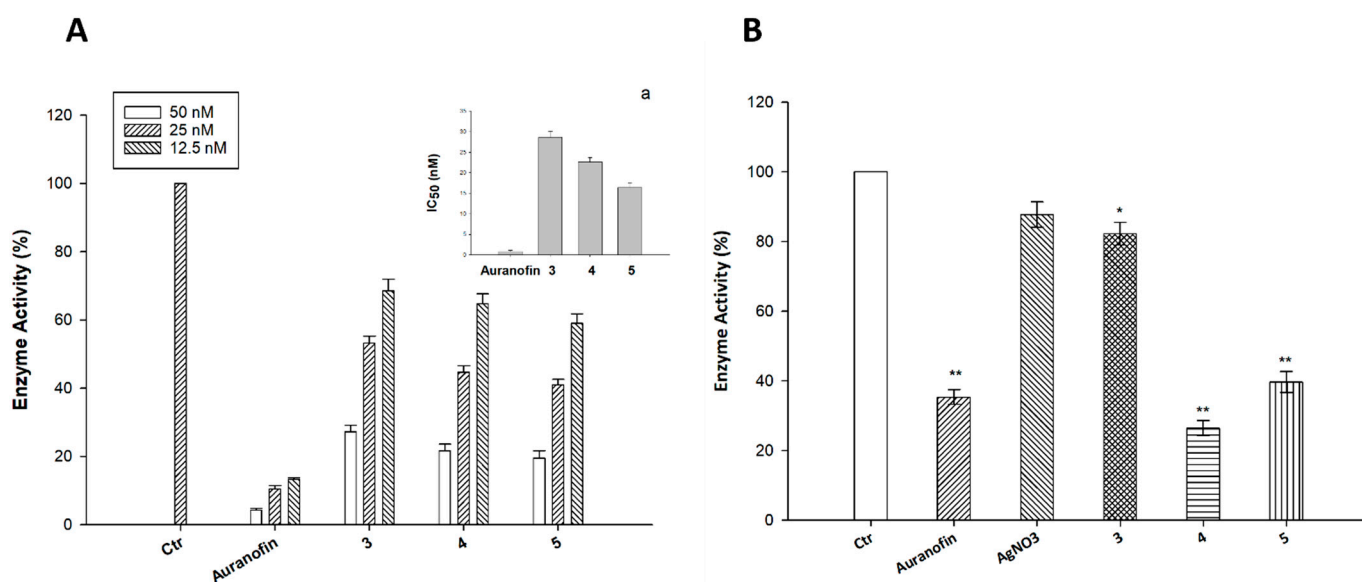


**Figure 2.** TrxR inhibition. (A) TrxR1 activity was assayed by measuring NADPH-dependent reduction of DTNB at 412 nm as described in the Experimental Section. (a) 50% inhibition concentration (IC<sub>50</sub>), Error bars indicate S.D. (B) U1285 cells were incubated for 24 h with the tested compounds (2 μM). Subsequently, cells were washed twice with PBS and lysed. TrxR activity was tested by measuring NADPH-dependent reduction of DTNB at 412 nm. Error bars indicate SD. \*  $p < 0.05$ ; \*\*  $p < 0.01$ .

On the other hand, Ag(I) compounds 4 and 5 were as effective or even better than auranofin in hampering TrxR activity when tested in U1285 cell cultures. Actually, derivative 4 tested at 2 μM was able to decrease TrxR enzyme activity by about 68%, compared with auranofin, which at the same concentration, induced a 62% inhibition of the Sec-containing redox enzyme (Figure 2B). These results clearly confirmed the ability of Ag(I) complexes to target TrxR in intact cancer cells.

It is widely known that Trx system plays an essential role in cellular redox homeostasis, and inhibition of this redox regulatory system has been shown to determine cellular redox unbalance in terms of sulfhydryl redox status and cellular production of reactive oxygen species (ROS) [61–63].

Hence, the effect induced by the newly developed heteroleptic Ag(I) complexes on total cellular sulfhydryl content and on ROS production was assayed in U1285-treated cells. As evident in Figure 3A, although to a different extent, all three silver(I) complexes were effective in modulating total thiol content of U1285 cells in a dose-dependent manner. In particular, the reduction of cellular sulfhydryl content obtained with **4** at the higher concentration tested (3  $\mu$ M) was very similar to that induced by equidoses of auranofin.

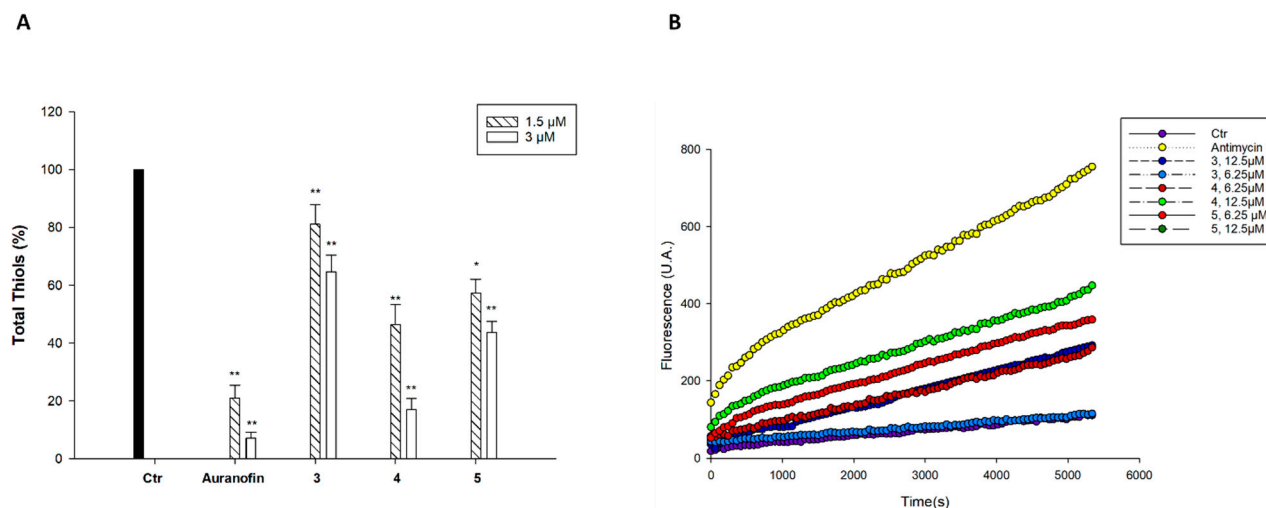


**Figure 3.** Effects on sulfhydryl content and ROS production. (A) Sulfhydryl content in U1285-treated cancer cells incubated for 24 h with tested compounds. The sulfhydryl group amount was determined by the DTNB assay. Error bars indicate S.D. \*  $p < 0.05$ , \*\*  $p < 0.01$ . (B) Effect of silver(I) compounds on hydrogen peroxide formation in U1285 cells. Cells were pre-incubated in PBS/10 mM glucose medium for 20 min at 37 °C in the presence of 10  $\mu$ M CM-DCFDA and then treated with increasing concentrations of the tested compounds.

Consistently, treatment of U1285 cells with Ag(I) complexes determined a substantial time-dependent and dose-dependent increase in cellular basal hydrogen peroxide production (Figure 3B), which was, however, less pronounced with respect to that elicited by antimycin, a classic inhibitor of the mitochondrial respiratory chain at the level of complex III.

Mitochondria are considered the main cellular source of ROS, and the magnitude of a change in mitochondrial ROS production strictly depends on the physicochemical state of this organelle. A persistent increase in the rate of ROS production and the induction of thiol redox stress are consistent with the collapse of mitochondrial shape and integrity (swelling), ultimately leading to the induction of cell apoptosis [64]. We therefore evaluated the effect determined by treatment with our newly synthesized Ag(I) complexes in terms of modification of mitochondrial pathophysiological characteristics, such as mitochondrial membrane potential and morphological changes, in SCLC cells.

For MMP detection, U1285 cells were treated with increasing concentrations of the tested complexes, and the percentage of cells with hypopolarized mitochondrial membrane potential was determined by means of the Mito-ID<sup>®</sup> Membrane Potential Kit. The carbonyl cyanide-*m*-chlorophenylhydrazone (CCCP) was used as positive control. Results depicted in Figure 4A show that the percentage of hypopolarized cells induced by treatment with tested complexes was dose-dependent and reached about 30% for compound **4** at the highest tested doses. Again, the L<sup>2OMe</sup>-bearing complexes **4** and **5** were those eliciting the highest effect, in accordance with all the above-reported results.



In agreement, TEM analyses performed on U1285 cells treated for 24 h with  $IC_{50}$  concentrations of the representative complexes 4 and 5 showed a dramatic swelling of the mitochondria, associated with a decrease in the electron density of the inner membrane and matrix regions, as clear signs of their antimitchondrial effect, thus confirming that they elicited a substantial modification of the mitochondria physiology (see Figure 4B).

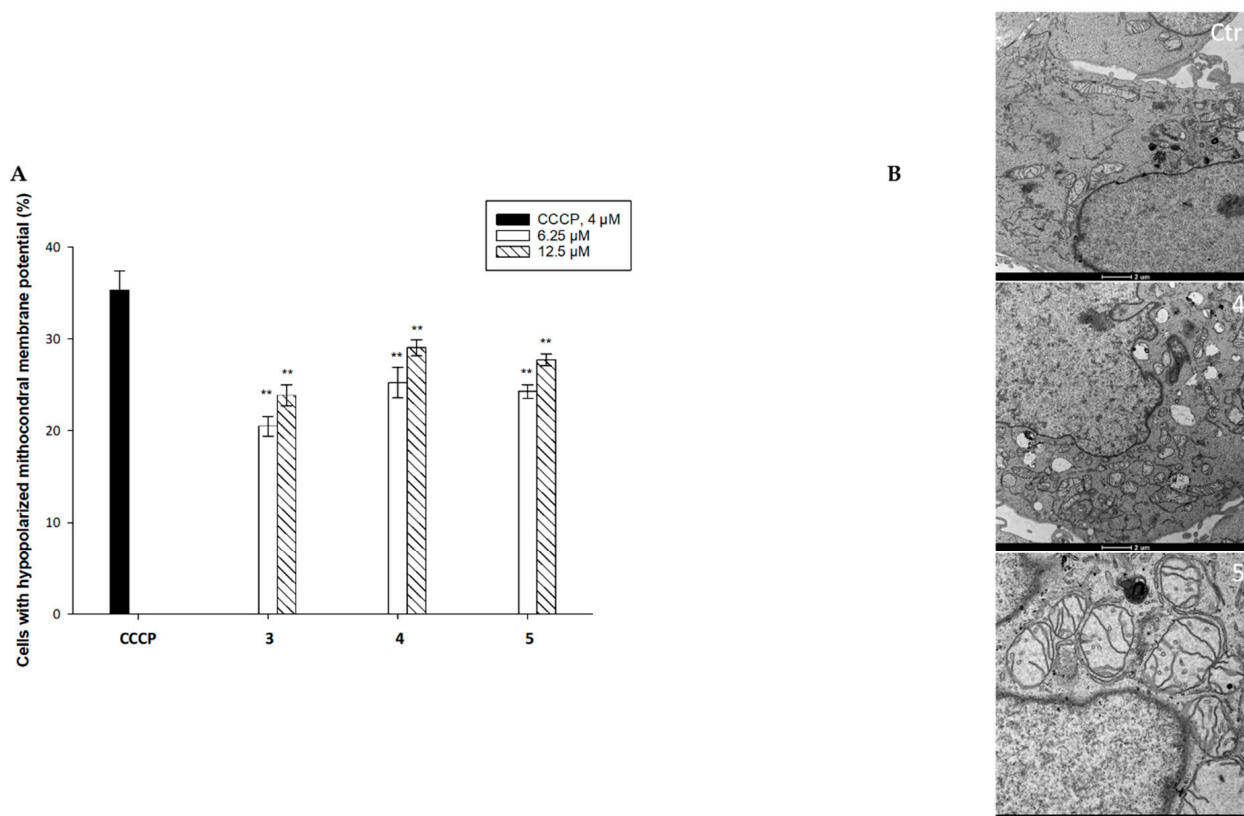


**Figure 4.** Antimitchondrial effect. (A) U1285 cells were treated for 24 h with increasing concentrations of the tested complexes or CCCP (3  $\mu$ M). The percentage of cells with hypopolarized mitochondrial membrane potential was determined by Mito-ID<sup>®</sup> Membrane Potential Kit. \*\*  $p \leq 0.01$ . Error bars indicate S.D. (B) TEM analysis. Transmission electron micrographs of untreated U1285 cells or 24 h treated cells with  $IC_{50}$  concentrations of complex 3 or complex 4.

Finally, owing to the well-established connection between oxidative stress and apoptosis induction, we assessed the ability of tested complexes to induce cancer cell death by triggering apoptosis. Figure 5 shows the results obtained upon monitoring cellular morphological changes in U1285 cells treated for 48 h with  $IC_{50}$  doses of 3–5 and stained with Hoechst 33258 fluorescent probe. Compared with control cells, cells treated with the tested complexes presented brightly stained nuclei and morphological features typical of cells undergoing apoptosis, such as chromatin condensation, thus confirming the ability of the newly developed Ag(I) complexes to induce apoptotic cell death in U1285 cells.

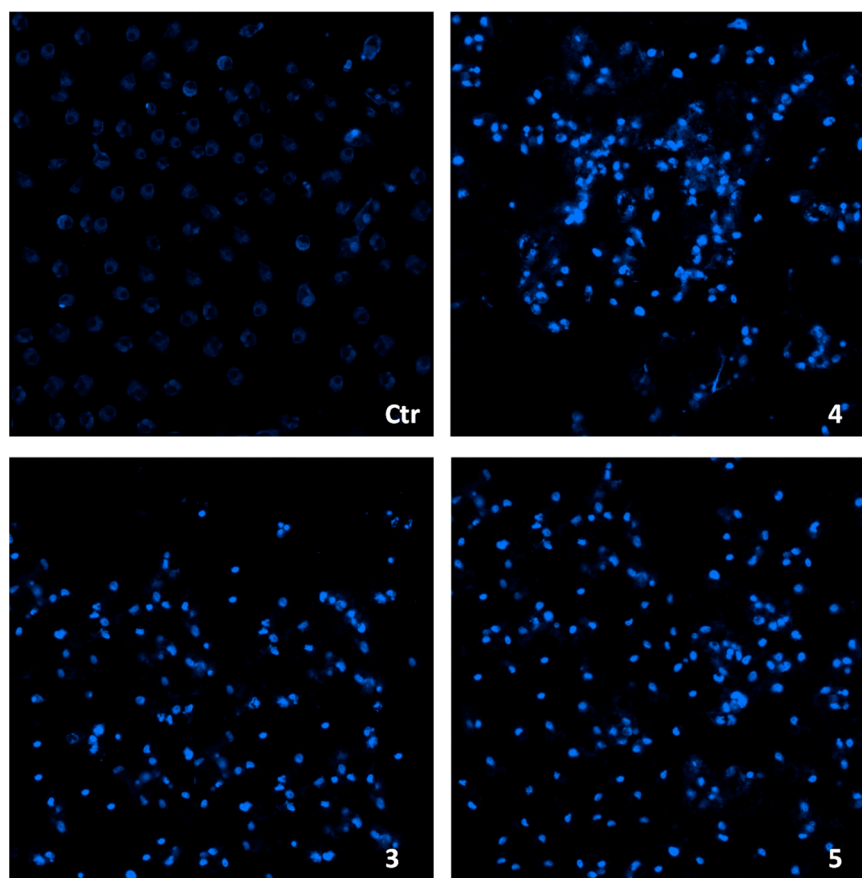


**Figure 5.** Hoechst staining (magnification,  $\times 20$ ) of U1285 cells incubated for 48 h with IC<sub>50</sub> doses of 3–5.

### 3. Materials and Methods

#### 3.1. Chemistry

##### 3.1.1. Materials and General Methods

All reagents were purchased and used without further purification. All solvents were dried, degassed, and distilled prior to use. Melting points were performed by an SMP3 Stuart Scientific Instrument (Bibby Sterilin Ltd., London, UK). Elemental analyses (C, H, N, S) were performed with a Fisons Instruments EA-1108 CHNS-O Elemental Analyzer (Thermo Fisher Scientific Inc., Waltham, MA, USA). Fourier-transform infrared (FT-IR) spectra were recorded from 4000 to 200  $\text{cm}^{-1}$  on a PerkinElmer Frontier Instrument (PerkinElmer Inc., Waltham, MA, USA), equipped with Attenuated Total Reflection (ATR) unit using universal diamond top-plate as sample holder. Abbreviation used in the analyses of the FT-IR spectra: m = medium, mbr = medium broad, s = strong, sbr = strong broad, sh = shoulder, vs = very strong, w = weak, wbr = weak broad.  $^1\text{H}$ -,  $^{13}\text{C}$ - and  $^{31}\text{P}$ -NMR spectra were recorded with a Bruker 500 Ascend Spectrometer (Bruker BioSpin Corporation, Billerica, MA, USA; 500.1 MHz for  $^1\text{H}$ , 125 MHz for  $^{13}\text{C}$  and 202.4 MHz for  $^{31}\text{P}$ ). Referencing was relative to tetramethylsilane (TMS) ( $^1\text{H}$  and  $^{13}\text{C}$ ) and 85%  $\text{H}_3\text{PO}_4$  ( $^{31}\text{P}$ ). NMR annotations used were as follows: br = broad, d = doublet, dbr = doublet broad, m = multiplet, mbr = multiplet broad, s = singlet, sbr = singlet broad, sept = septet, t = triplet. Electrospray ionization mass spectra (ESI-MS) were recorded in positive- (ESI-MS(+)) or negative-ions (ESI-MS(−)) mode on a Waters Micromass ZQ Spectrometer equipped with a single quadrupole (Waters Corporation, Milford, MA, USA), using a methanol or acetonitrile mobile phase. The compounds were added to reagent-grade methanol or acetonitrile to give approximately 0.1 mM solutions. These solutions were injected (1  $\mu\text{L}$ ) into the spectrometer fitted with an autosampler. The pump delivered the solutions to the mass spectrometer source at a flow rate of 200  $\mu\text{L}/\text{min}$ , and nitrogen was employed both as a drying and nebulizing

gas. Capillary voltage was typically 2500 V. The temperature of the source was 100 °C, while the temperature of the desolvation was 400 °C. In the analyses of ESI-MS spectra, the confirmation of major peaks was supported by comparison of the observed and predicted isotope distribution patterns, the latter calculated using the IsoPro 3.1 computer software (T-Tech Inc., Norcross, GA, USA). The electrical conductivity of the acetonitrile and dimethyl sulfoxide solutions was measured with a Crison CDTM 522 conductivity meter (Crison Instruments SA, Barcelona, Spain) at room temperature.

The precursors HC(pz)<sub>2</sub>COOH (LH) [27] and HC(pz<sup>Me2</sup>)<sub>2</sub>COOH (L<sup>2</sup>H) [26] were prepared by literature method. The ligands [HC(pz)<sub>2</sub>COOCH<sub>3</sub>] (L<sup>OMe</sup>, **1**) [65] and [HC(pz<sup>Me2</sup>)<sub>2</sub>COOCH<sub>3</sub>] (L<sup>2OMe</sup>, **2**) were prepared by literature method [66] and were fully characterized (<sup>1</sup>H-NMR: Figures S2 and S3).

### 3.1.2. Synthesis of [Ag(PPh<sub>3</sub>)(L<sup>OMe</sup>)]NO<sub>3</sub> (**3**)

AgNO<sub>3</sub> (1.000 mmol, 0.170 g) was added to a solution of triphenylphosphine (PPh<sub>3</sub>, 1.000 mmol, 0.262 g) in methanol (30 mL). The reaction mixture was stirred at room temperature for 3 h; then, ligand **1** (1.000 mmol, 0.206 g) was added, and the solution was stirred for 24 h at room temperature in the dark. The solution was dried at reduced pressure, and the residue was recrystallized by diethyl ether to give the whitish complex **3** in 90% yield. M.p.: 165–168 °C.  $\Lambda_0$  (CH<sub>3</sub>CN, 10<sup>-3</sup> M, 293 K): 134 Ω<sup>-1</sup> cm<sup>2</sup> mol<sup>-1</sup>. FT-IR (cm<sup>-1</sup>) (Figure S4): 3117wbr, 3058wbr, 2938wbr, 2886wbr, 2849wbr (C-H); 1760s (C=O); 1523wbr, 1480m, 1454m (C=C/C=N); 1436m, 1398s, 1379m; 1314s, 1299s, 1283s (NO<sub>3</sub>); 1257m, 1228s, 1207m, 1182m, 1159m, 1095s, 1062m, 1039m, 1027m, 999m, 983m, 972m, 919m, 900m, 851m, 825m, 810m, 763s, 748vs, 707m, 694s, 656m, 617m, 597m, 523s, 493s, 437w, 403w, 365w, 346w, 331m, 281w, 250w, 228w, 210m. <sup>1</sup>H-NMR (CD<sub>3</sub>CN, 293 K, Figure S5): δ 3.69 (s, 3H, OCH<sub>3</sub>), 6.42 (t, <sup>3</sup>J<sub>HH</sub> = 6.4 Hz, 2H, 4-CH), 7.46-7.58 (m, 16H, CHCO and CH<sub>ar</sub>), 7.65 (d, <sup>3</sup>J<sub>HH</sub> = 7.7 Hz, 2H, 5-CH), 7.96 (d, <sup>3</sup>J<sub>HH</sub> = 8.0 Hz, 2H, 3-CH). <sup>1</sup>H-NMR (CDCl<sub>3</sub>, 293 K): δ 3.75 (s, 3H, OCH<sub>3</sub>), 6.36 (t, <sup>3</sup>J<sub>HH</sub> = 6.4 Hz, 2H, 4-CH), 7.48-7.55 (m, 16H, CHCO and CH<sub>ar</sub>), 7.59 (d, <sup>3</sup>J<sub>HH</sub> = 7.6 Hz, 2H, 5-CH), 8.25 (d, <sup>3</sup>J<sub>HH</sub> = 8.3 Hz, 2H, 3-CH). <sup>13</sup>C{<sup>1</sup>H}-NMR (CD<sub>3</sub>CN, 293 K, Figure S6): δ 53.46, 73.30, 106.99, 129.21, 129.29, 130.99, 131.01, 131.23, 131.97, 133.72, 141.86, 164.94. <sup>31</sup>P{<sup>1</sup>H}-NMR (CD<sub>3</sub>CN, 293 K): δ 10.67 (br). <sup>31</sup>P{<sup>1</sup>H}-NMR (CD<sub>3</sub>CN, 243 K, Figure S7): δ 10.79 (d, <sup>1</sup>J(<sup>107</sup>Ag-<sup>31</sup>P) = 624 Hz and d, <sup>1</sup>J(<sup>109</sup>Ag-<sup>31</sup>P) = 722 Hz). <sup>31</sup>P{<sup>1</sup>H}-NMR (CDCl<sub>3</sub>, 293 K): δ 16.87 (d, <sup>1</sup>J(Ag-<sup>31</sup>P) = 671 Hz). <sup>31</sup>P{<sup>1</sup>H}-NMR (CDCl<sub>3</sub>, 243 K): δ 16.09 (d, <sup>1</sup>J(<sup>107</sup>Ag-<sup>31</sup>P) = 662 Hz; d, <sup>1</sup>J(<sup>109</sup>Ag-<sup>31</sup>P) = 749 Hz). <sup>31</sup>P{<sup>1</sup>H}-NMR (CD<sub>3</sub>OD, 293 K): δ 13.95 (d, <sup>1</sup>J(Ag-<sup>31</sup>P) = 723 Hz). <sup>31</sup>P{<sup>1</sup>H}-NMR (CD<sub>3</sub>OD, 223 K, Figure S8): δ 12.01 (d, <sup>1</sup>J(<sup>107</sup>Ag-<sup>31</sup>P) = 642 Hz; d, <sup>1</sup>J(<sup>109</sup>Ag-<sup>31</sup>P) = 742 Hz). ESI-MS (major positive ions, CH<sub>3</sub>CN), *m/z* (%): 313 (20) [Ag(L<sup>OMe</sup>)]<sup>+</sup>, 371 (25) [Ag(PPh<sub>3</sub>)]<sup>+</sup>, 577 (100) [Ag(PPh<sub>3</sub>)(L<sup>OMe</sup>)]<sup>+</sup>, 633 (50) [Ag(PPh<sub>3</sub>)<sub>2</sub>]<sup>+</sup>. ESI-MS (major negative ions, CH<sub>3</sub>CN), *m/z* (%): 231 (100) [Ag(NO<sub>3</sub>)<sub>2</sub>]<sup>-</sup>. Elemental analysis (%) calculated for C<sub>27</sub>H<sub>25</sub>AgN<sub>5</sub>O<sub>5</sub>P: C 50.80, H 3.95, N 10.97; found: C 50.81, H 3.95, N 10.80.

### 3.1.3. Synthesis of [Ag(PPh<sub>3</sub>)(L<sup>2OMe</sup>)]NO<sub>3</sub> (**4**)

This compound was prepared following the procedure described for **3**, using ligand **2** (1.000 mmol, 0.262 g), to give the whitish complex **4** in 89% yield. M.p.: 188–193 °C.  $\Lambda_0$  (CH<sub>3</sub>CN, 10<sup>-3</sup> M, 293 K): 135 Ω<sup>-1</sup> cm<sup>2</sup> mol<sup>-1</sup>. FT-IR (cm<sup>-1</sup>) (Figure S9): 3136wbr, 3051wbr, 2956wbr, 2921wbr (C-H); 1760s (C=O); 1561m, 1471mbr (C=C/C=N); 1436m, 1420m; 1380mbr, 1323sbr, 1299s, 1270m (NO<sub>3</sub>); 1221m, 1185m, 1154wbr, 1124wbr, 1112wbr, 1097m, 1073wbr, 1032mbr, 999mbr, 976sh, 918w, 891m, 870m, 824m, 803m, 782m, 757m, 743s, 720m, 694s, 639w, 603w, 523s, 503m, 488m, 447m, 422w, 391w, 367w, 281w, 269w, 235w, 224m, 204m. <sup>1</sup>H-NMR (CD<sub>3</sub>CN, 293 K, Figure S10): δ 2.17 (s, 6H, 3- or 5-CH<sub>3</sub>), 2.46 (s, 6H, 3- or 5-CH<sub>3</sub>), 3.42 (s, 3H, OCH<sub>3</sub>), 6.12 (s, 2H, 4-CH), 7.04 (s, 1H, CHCO), 7.50-7.59 (m, 15H, CH<sub>ar</sub>). <sup>1</sup>H-NMR (CDCl<sub>3</sub>, 293 K): δ 2.09 (s, 6H, 3-CH<sub>3</sub>), 2.55 (s, 6H, 5-CH<sub>3</sub>), 3.75 (s, 3H, OCH<sub>3</sub>), 5.97 (s, 2H, 4-CH), 7.49-7.51 (m, 16H, CHCO and CH<sub>ar</sub>). <sup>13</sup>C{<sup>1</sup>H}-NMR (CD<sub>3</sub>CN, 293 K, Figure S11): δ 10.31, 13.53, 53.53, 66.60, 106.63, 129.25, 131.07, 131.55, 133.68, 143.50, 151.38, 164.96. <sup>31</sup>P{<sup>1</sup>H}-NMR (CD<sub>3</sub>CN, 293 K): δ 12.74 (dbr, <sup>1</sup>J(Ag-<sup>31</sup>P) = 626 Hz). <sup>31</sup>P{<sup>1</sup>H}-NMR

(CD<sub>3</sub>CN, 243 K, Figure S12):  $\delta$  11.26 (d,  $^1J(^{107}\text{Ag}-^{31}\text{P}) = 611$  Hz; d,  $^1J(^{109}\text{Ag}-^{31}\text{P}) = 705$  Hz).  $^{31}\text{P}\{^1\text{H}\}$ -NMR (CDCl<sub>3</sub>, 293 K):  $\delta$  16.03 (dbr,  $^1J(\text{Ag}-^{31}\text{P}) = 683$  Hz).  $^{31}\text{P}\{^1\text{H}\}$ -NMR (CDCl<sub>3</sub>, 223 K, Figure S13):  $\delta$  12.03 (d,  $^1J(^{107}\text{Ag}-^{31}\text{P}) = 628$  Hz; d,  $^1J(^{109}\text{Ag}-^{31}\text{P}) = 725$  Hz). ESI-MS(+) (major positive ions, CH<sub>3</sub>CN),  $m/z$  (%): 371 (15) [Ag(PPh<sub>3</sub>)<sup>+</sup>, 633 (100) [Ag(PPh<sub>3</sub>)(L<sup>2OMe</sup>)<sup>+</sup>. ESI-MS(-) (major negative ions, CH<sub>3</sub>CN),  $m/z$  (%): 231 (100) [Ag(NO<sub>3</sub>)<sub>2</sub>]<sup>-</sup>. Elemental analysis (%) calculated for C<sub>31</sub>H<sub>33</sub>AgN<sub>5</sub>O<sub>5</sub>P: C 53.61, H 4.79, N 10.08; found: C 53.68, H 4.84, N 9.93.

### 3.1.4. Synthesis of [Ag(PTA)(L<sup>2OMe</sup>)]NO<sub>3</sub> (5)

AgNO<sub>3</sub> (1.000 mmol, 0.170 g) was added to a solution of 1,3,5-triaza-7-phosphaadamantane (PTA, 1.000 mmol, 0.157 g) in methanol (30 mL). The reaction mixture was stirred at room temperature for 3 h; then, ligand **2** (1.000 mmol, 0.262 g) was added, and the solution was stirred for 24 h at room temperature in the dark. The solution was dried at reduced pressure, and the residue was recrystallized by diethyl ether to give the whitish complex **5** in 78% yield. M.p.: 210–214 °C.  $\Lambda_0$  (DMSO, 10<sup>-3</sup> M, 293 K): 25  $\Omega^{-1}$  cm<sup>2</sup> mol<sup>-1</sup>. FT-IR (cm<sup>-1</sup>) (Figure S14): 3137wbr, 2958wbr, 2920wbr, 2852wbr (C-H); 1760m (C=O); 1642w; 1561w (C=C/C=N); 1447wbr, 1419m, 1395m, 1385m, 1367m; 1320mbr, 1296mbr (NO<sub>3</sub>); 1264m, 1241m; 1220m, 1155w, 1126w, 1107w, 1099w, 1036w, 1013mbr, 973m, 950m, 890w, 866w, 810m, 791m, 782mbr, 753wbr, 710m, 639m, 605m, 580m, 565m, 484m, 454m, 397m, 349m, 280m, 251m, 209m. <sup>1</sup>H-NMR (CD<sub>3</sub>CN, 293 K, Figure S15):  $\delta$  2.20 (s, 6H, 3-CH<sub>3</sub>), 2.38 (s, 6H, 5-CH<sub>3</sub>), 3.78 (s, 3H, OCH<sub>3</sub>), 4.35 (sbr, 6H, NCH<sub>2</sub>P), 4.53–4.67 (m, 6H, NCH<sub>2</sub>N), 6.06 (s, 2H, 4-CH), 6.95 (s, 1H, CHCO). <sup>13</sup>C{<sup>1</sup>H}-NMR (CD<sub>3</sub>CN, 293 K, Figure S16):  $\delta$  10.27, 13.37, 50.60, 53.61, 67.23, 72.57, 106.53, 143.15, 150.88, 164.91.  $^{31}\text{P}\{^1\text{H}\}$ -NMR (CD<sub>3</sub>CN, 293 K):  $\delta$  -84.87 (sbr).  $^{31}\text{P}\{^1\text{H}\}$ -NMR (CD<sub>3</sub>CN, 243 K, Figure S17):  $\delta$  -86.11 (d,  $^1J(^{107}\text{Ag}-^{31}\text{P}) = 609$  Hz; d,  $^1J(^{109}\text{Ag}-^{31}\text{P}) = 698$  Hz).  $^{31}\text{P}\{^1\text{H}\}$ -NMR (CD<sub>3</sub>OD, 293 K):  $\delta$  -82.11 (sbr).  $^{31}\text{P}\{^1\text{H}\}$ -NMR (CD<sub>3</sub>OD, 223 K):  $\delta$  -81.26 (d,  $^1J(^{107}\text{Ag}-^{31}\text{P}) = 624$  Hz; d,  $^1J(^{109}\text{Ag}-^{31}\text{P}) = 698$  Hz). ESI-MS(+) (major positive ions, CH<sub>3</sub>CN),  $m/z$  (%): 158 (20) [PTA + H]<sup>+</sup>, 264 (5) [Ag(PTA)]<sup>+</sup>, 371 (30) [Ag(L<sup>2OMe</sup>)]<sup>+</sup>, 528 (100) [Ag(PTA)(L<sup>2OMe</sup>)]<sup>+</sup>, 633 (50) [Ag(L<sup>2OMe</sup>)<sub>2</sub>]<sup>+</sup>. ESI-MS(-) (major negative ions, CH<sub>3</sub>CN),  $m/z$  (%): 62 (100) [NO<sub>3</sub>]<sup>-</sup>, 231 (10) [Ag(NO<sub>3</sub>)<sub>2</sub>]<sup>-</sup>. Elemental analysis (%) calculated for C<sub>19</sub>H<sub>30</sub>AgN<sub>8</sub>O<sub>5</sub>P: C 39.42, H 5.13, N 19.01; found: C 40.00, H 5.32, N 19.51.

### 3.1.5. Stability Studies in DMSO/RPMI

All complexes were dissolved at 50  $\mu\text{M}$  in 0.5% DMSO/RPMI. UV-Vis spectra were recorded at  $t = 0$  min,  $t = 24$  h,  $t = 48$  and  $t = 72$  h by a Perkin-Elmer Lambda 25 (Perkin-Elmer).

## 3.2. Experiments with Cultured Human Cancer Cells

Ag(I) complexes and the corresponding uncoordinated ligands were dissolved in DMSO just before the experiment, and a calculated amount of drug solution was added to the cell growth medium to a final solvent concentration of 0.5%, which had no detectable effects on cell viability. Cisplatin was dissolved in 0.9% sodium chloride solution. MTT (3-(4,5-dimethylthiazol-2-yl)-2,5-diphenyltetrazolium bromide) and cisplatin were obtained from Sigma Chemical Co, St. Louis, MO, USA.

### 3.2.1. Cell Cultures

Human SCLC (U1285), breast (MDA-MB-231), colon (HCT-15), and pancreatic (PSN-1) carcinoma cell lines were obtained by American Type Culture Collection (ATCC, Rockville, MD, USA). A431 are human cervical carcinoma cells kindly provided by Professor F. Zunino (Division of Experimental Oncology B, Istituto Nazionale dei Tumori, Milan, Italy). The 2008 cells and the cisplatin-resistant variant, C13\* cells, are human ovarian adenocarcinoma cell lines that were kindly provided by Professor G. Marverti (Department of Biomedical Science of Modena University, Modena, Italy). Cell lines were maintained in the logarithmic phase at 37 °C in a 5% carbon dioxide atmosphere using the following culture media containing 10% fetal calf serum (EuroClone, Milan, Italy), antibiotics (50 units/mL penicillin

and 50 µg/mL streptomycin) and 2 mM l-glutamine: (i) RPMI-1640 medium (EuroClone, Milan, Italy) for HCT-15, A431, PSN-1, U1285, 2008 and C13\* cells; (ii) DMEM (EuroClone, Milan, Italy) for MDA-MB-231 cells.

### 3.2.2. MTT Assay

The growth inhibitory effect toward tumor cells was evaluated by means of MTT assay. Briefly,  $3\text{--}8 \times 10^3$  cells/well, dependent upon the growth characteristics of the cell line, were seeded in 96-well microplates in growth medium (100 µL). After 24 h, the medium was removed and replaced with a fresh one containing the compound to be studied at the appropriate concentration. Triplicate cultures were established for each treatment. After 72 h, each well was treated with 10 µL of a 5 mg/mL MTT saline solution, and following 5 h of incubation, 100 µL of a sodium dodecyl sulfate (SDS) solution in HCl 0.01 M was added. After overnight incubation, cell growth inhibition was detected by measuring the absorbance of each well at 570 nm using a Bio-Rad 680 microplate reader. Mean absorbance for each drug dose was expressed as a percentage of the control untreated well absorbance and plotted vs. drug concentration.  $IC_{50}$  values, the drug concentrations that reduce the mean absorbance at 570 nm to 50% of those in the untreated control wells, were calculated by the four-parameter logistic (4-PL) model. Evaluation was based on means from at least four independent experiments.

### 3.2.3. Spheroid Cultures

Spheroid cultures were obtained by seeding  $2.5 \times 10^3$  U1285 cancer cells/well in a round-bottom non-treated tissue culture 96-well plate (Greiner Bio-one, Kremsmünster, Austria) in phenol red free RPMI-1640 medium (Sigma Chemical Co., St. Louis, MO, USA) containing 10% fetal calf serum and supplemented with 20% methyl cellulose stock solution.

### 3.2.4. Acid Phosphatase (APH) Assay

An APH modified assay was used for determining cell viability in 3D spheroids, as previously described [67]. Briefly, the pre-seeded spheroids were treated with fresh medium containing the compound to be studied at the appropriate concentration (range 5–150 µM). Triplicate cultures were established for each treatment. After 72 h, each well was treated with 100 µL of the assay buffer (0.1 M sodium acetate, 0.1% Triton-X-100, supplemented with ImmunoPure p-nitrophenyl phosphate; Sigma Chemical Co., St. Louis, MO, USA), and following 3 h of incubation, 10 µL of 1 M NaOH solution was added. The inhibition of the cell growth induced by the tested complexes was detected by measuring the absorbance of each well at 405 nm, using a Bio-Rad 680 microplate reader. Mean absorbance for each drug dose was expressed as a percentage of the control untreated well absorbance (T/C) and plotted vs. drug concentration.  $IC_{50}$  values, the drug concentrations that reduce the mean absorbance at 405 nm 50% of those in the untreated control wells, were calculated by four-parameter logistic (4-PL) model. Evaluation was based on means from at least four independent experiments.

### 3.2.5. Cellular Uptake

U1285 cells ( $2.5 \times 10^6$ ) were seeded in 75 cm<sup>2</sup> flasks in growth medium (20 mL). After 24 h, the medium was replaced, and the cells were incubated for 24 h with tested complexes. Monolayers were then washed twice with ice-cold phosphate-buffered saline (PBS), harvested, and counted. Cell samples were subjected to five freeze–thaw cycles at  $-80$  °C and then vigorously vortexed. The samples were treated with highly pure nitric acid (1 mL;  $Ag < 0.01 \mu\text{gkg}^{-1}$ ) and transferred into a microwave Teflon vessel. Samples were then submitted to standard mineralization procedures and analyzed for the silver amount by using a Varian AA Duo graphite furnace atomic absorption spectrometer (Varian, Palo Alto, CA; USA) at 242.795 nm. The calibration curve was obtained using known concentrations of standard solutions purchased from Sigma Chemical Co., St. Louis, MO, USA.



### 3.2.6. TrxR Inhibition

Cell-free studies: the assay was performed in PBS buffer pH 7.4, containing 5 mM EDTA, 0.250 mM nicotinamide adenine dinucleotide phosphate (NADPH) and 75 nmol of TrxR1 (Sigma Chemical Co., St. Louis, MO, USA). The silver(I) complexes as well as auranofin were pre-incubated for 5 min at room temperature; the reaction was started with 1 mM DTNB (5,5'-dithiobis(2-nitrobenzoic acid)), and the increase in absorbance was monitored at 412 nm over 5 min at 25 °C. Enzyme activity was calculated taking into account that 1 mol of NADPH yields 2 mol of CNTP anion (carboxy-nitro-thiophenol, reduced DTNB).

Cellular studies: U1285 cells were grown in 75 cm<sup>2</sup> flasks at confluence and treated with Ag(I) complexes at concentrations corresponding to IC<sub>50</sub> values for 18 h. At the end of incubation time, cells were collected, washed with ice-cold PBS and centrifuged at ×g. Each sample was then lysed with RIPA buffer modified as follows: 150 mM NaCl, 50 mM Tris-HCl, 1% Triton X-100, 1% SDS, 1% DOC, 1 mM NaF, 1 mM EDTA, and immediately before use, an anti-protease cocktail (Roche, Basel, Switzerland) containing PMSF was added. Samples were tested for TrxR activity as above described.

### 3.2.7. Quantification of Thiols

U1285 cells ( $2 \times 10^5$ ) were seeded in a six-well plate in growth medium (4 mL). After 24 h, cells were incubated for 36 h with IC<sub>50</sub> concentrations of tested compounds. Subsequently, the thiol content was measured as previously described [68].

### 3.2.8. Reactive Oxygen Species Production

The production of ROS was measured in U1285 cells ( $10^4$  per well) grown for 24 h in a 96-well plate in RPMI medium without phenol red (Sigma Chemical Co., St. Louis, MO, USA). Cells were then washed with ice-cold PBS and loaded with 10 μM 5-(and-6)-chloromethyl-2',7'-dichlorodihydrofluorescein diacetate acetyl ester (CM-H<sub>2</sub>DCFDA) (Molecular Probes-Invitrogen, Eugene, OR, USA) for 25 min in the dark. Afterward, cells were washed with PBS and incubated with tested compounds. Fluorescence increase was estimated utilizing the wavelengths of 485 (excitation) and 527 nm (emission) in an Infinite<sup>®</sup> 200 PRO (Tecan, Switzerland) plate reader. Antimycin (3 μM, Sigma Chemical Co., St. Louis, MO, USA), a potent inhibitor of Complex III in the electron transport chain, and auranofin were used as positive controls.

### 3.2.9. Mitochondrial Membrane Potential ( $\Delta\Psi$ )

The  $\Delta\Psi$  was assayed using the Mito-ID<sup>®</sup> Membrane Potential Kit according to the manufacturer's instructions (Enzo Life Sciences, Farmingdale, NY, USA). Briefly, U1285 cells ( $8 \times 10^3$  per well) were seeded in 96-well plates; after 24 h, cells were washed with PBS and loaded with Mito-ID Detection Reagent for 30 min at 37 °C in the dark. Afterward, cells were incubated with increasing concentrations of tested complexes. Fluorescence intensity was estimated using a plate reader (Fluoroskan Ascent FL, Labsystems, Finland) at 490 (excitation) and 590 nm (emission). Carbonyl cyanide m-chlorophenyl hydrazone (CCCP, 4 μM), a chemical inhibitor of the oxidative phosphorylation, was used as a positive control.

### 3.2.10. TEM Analysis

About  $10^6$  U1285 cells were seeded in 24-well plates and, after 24 h incubation, were treated with IC<sub>50</sub> concentrations of tested compounds and incubated for additional 24 h. Cells were then washed with cold PBS, harvested and directly fixed with 1.5% glutaraldehyde buffer with 0.2 M sodium cacodylate, pH 7.4. After washing with buffer and postfixation with 1% OsO<sub>4</sub> in 0.2 M cacodylate buffer, specimens were dehydrated and embedded in epoxy resin (Epon Araldite). Sagittal serial sections (1 μm) were counterstained with toluidine blue; thin sections (90 nm) were given contrast by staining with uranyl acetate and lead citrate. Micrographs were taken with a Hitachi H-600 electron microscope (Hitachi, Tokyo, Japan) operating at 75 kV. All photos were typeset in Corel Draw 11.

### 3.2.11. Cell Death Induction

U1285 cells were seeded into 8-well tissue-culture slides (BD Falcon, Bedford, MA, USA) at  $5 \times 10^4$  cells/well ( $0.8 \text{ cm}^2$ ). After 24 h, the cells were washed twice with PBS, and following 48 h of treatment with  $\text{IC}_{50}$  doses of the tested compound, cells were stained for 5 min with  $10 \text{ }\mu\text{g/mL}$  of Hoechst 33258 (20-(4-hydroxyphenyl)-5-(4-methyl-1-piperazinyl)-2,50-bi-1H-benzimidazole trihydrochloride hydrate, Sigma-Aldrich, St. Louis, MI, USA) in PBS. Samples were examined at  $5\times$  and  $40\times$  magnification in a Zeiss LSM 800 confocal microscope using the Zeiss ZEN 2.3 software system.

### 3.2.12. Statistical Analysis

All values are the means  $\pm$  v SD of no less than three measurements starting from three different cell cultures. Multiple comparisons were made by ANOVA followed by the Tukey–Kramer multiple comparison test ( $* p < 0.05$ ,  $** p < 0.01$ ), using GraphPad InStat software (GraphPad Software, San Diego, CA, USA).

## 4. Conclusions

The methyl ester derivatives  $\text{L}^{\text{OMe}}$  and  $\text{L}^{2\text{OMe}}$  of bis(pyrazol-1-yl)- and bis(3,5-dimethylpyrazol-1-yl)-acetic acid were synthesized and used for the preparation of the silver(I) complexes **3–5** following a one-pot synthesis in methanol. The lipophilic  $\text{PPh}_3$  and the hydrophilic PTA were selected as coligands to stabilize silver in +1 oxidation state. The compounds were fully characterized both in solid state and in solution.

All the investigated complexes showed significant cytotoxic effects against a panel of human cancer cell lines, with  $\text{IC}_{50}$  values in the low/sub-micromolar range, and proved to be more effective than the reference metaldrug cisplatin, especially when tested against the highly aggressive and intrinsically resistant SCLC cells, either in 2D or 3D cancer cell models. Mechanistic investigations of the cytotoxic effects demonstrated that the newly developed Ag(I) complexes induce an oxidative shift in the redox status of SCLC cells as well as a direct antimitochondrial effect due to their ability to target cellular TrxR. These results, besides supporting the hypothesis that TrxR represents a major cellular target for this class of complexes, suggest that TrxR inhibition by redox modulators, such as Ag(I) complexes, could represent a valuable strategy to target intrinsically refractory SCLC cells.

**Supplementary Materials:** The supporting information can be downloaded at: <https://www.mdpi.com/article/10.3390/ijms24044091/s1>.

**Author Contributions:** M.P. and C.S. designed the novel compounds reported in the manuscript and planned the synthetic procedures. L.B. and M.C. developed the chemical synthesis and characterized the ligands and the related complexes. M.P., C.S., C.M. and V.G. drafted the main text of the manuscript. P.S. and M.Z. performed the stability studies. V.G. and C.M. designed the biological studies. M.D.F. set up and performed all the biological assays. All authors have read and agreed to the published version of the manuscript.

**Funding:** This work was supported by Unione Europea—NextGenerationEU, “MUR-Fondo Promozione e Sviluppo—D.M. 737/2021, An innovative platform against SARS-CoV-2 and other emerging viruses grounded on copper-based materials (INVIRCuM)” (University of Camerino, FAR 2022 PNR) and the University of Padova (PRID BIRD225980). We are grateful to CIRCMSB (Consorzio Interuniversitario di Ricerca in Chimica dei Metalli nei Sistemi Biologici).

**Institutional Review Board Statement:** Not applicable.

**Informed Consent Statement:** Not applicable.

**Data Availability Statement:** The data presented in this study are available from the authors on request.

**Conflicts of Interest:** The authors declare no conflict of interest.

## References

1. Mjos, K.D.; Orvig, C. Metallo drugs in medicinal inorganic chemistry. *Chem. Rev.* **2014**, *114*, 4540–4563. [[CrossRef](#)] [[PubMed](#)]
2. Ceresa, C.; Bravin, A.; Cavaletti, G.; Pellei, M.; Santini, C. The combined therapeutical effect of metal-based drugs and radiation therapy: The present status of research. *Curr. Med. Chem.* **2014**, *21*, 2237–2265. [[CrossRef](#)] [[PubMed](#)]
3. Barry, N.P.E.; Sadler, P.J. Exploration of the medical periodic table: Towards new targets. *Chem. Commun.* **2013**, *49*, 5106–5131. [[CrossRef](#)] [[PubMed](#)]
4. Medici, S.; Peana, M.; Crisponi, G.; Nurchi, V.M.; Lachowicz, J.I.; Remelli, M.; Zoroddu, M.A. Silver coordination compounds: A new horizon in medicine. *Coord. Chem. Rev.* **2016**, *327–328*, 349–359. [[CrossRef](#)]
5. Porchia, M.; Pellei, M.; Marinelli, M.; Tisato, F.; Del Bello, F.; Santini, C. New insights in Au-NHCs complexes as anticancer agents. *Eur. J. Med. Chem.* **2018**, *146*, 709–746. [[CrossRef](#)]
6. Santini, C.; Pellei, M.; Gandin, V.; Porchia, M.; Tisato, F.; Marzano, C. Advances in copper complexes as anticancer agents. *Chem. Rev.* **2014**, *114*, 815–862. [[CrossRef](#)]
7. Nobili, S.; Mini, E.; Landini, I.; Gabbiani, C.; Casini, A.; Messori, L. Gold compounds as anticancer agents: Chemistry, cellular pharmacology, and preclinical studies. *Med. Res. Rev.* **2010**, *30*, 550–580. [[CrossRef](#)]
8. Tisato, F.; Marzano, C.; Porchia, M.; Pellei, M.; Santini, C. Copper in diseases and treatments, and copper-based anticancer strategies. *Med. Res. Rev.* **2010**, *30*, 708–749. [[CrossRef](#)]
9. Medici, S.; Peana, M.; Nurchi, V.M.; Zoroddu, M.A. Medical uses of silver: History, myths, and scientific evidence. *J. Med. Chem.* **2019**, *62*, 5923–5943. [[CrossRef](#)]
10. Medici, S.; Peana, M.; Nurchi, V.M.; Lachowicz, J.I.; Crisponi, G.; Zoroddu, M.A. Noble metals in medicine: Latest advances. *Coord. Chem. Rev.* **2015**, *284* (Suppl. C), 329–350. [[CrossRef](#)]
11. Rai, M.; Ingle, A.P.; Paralikar, P.; Gupta, I.; Medici, S.; Santos, C.A. Recent advances in use of silver nanoparticles as antimalarial agents. *Int. J. Pharm.* **2017**, *526*, 254–270. [[CrossRef](#)] [[PubMed](#)]
12. Liang, X.; Luan, S.; Yin, Z.; He, M.; He, C.; Yin, L.; Zou, Y.; Yuan, Z.; Li, L.; Song, X.; et al. Recent advances in the medical use of silver complex. *Eur. J. Med. Chem.* **2018**, *157*, 62–80. [[CrossRef](#)] [[PubMed](#)]
13. Marinelli, M.; Santini, C.; Pellei, M. Recent advances in medicinal applications of coinage-metal (Cu and Ag) N-Heterocyclic carbene complexes. *Curr. Trends Med. Chem.* **2016**, *16*, 2995–3017. [[CrossRef](#)] [[PubMed](#)]
14. McKeage, M.J.; Papathanasiou, P.; Salem, G.; Sjaarda, A.; Swiegers, G.F.; Waring, P.; Wild, S.B. Antitumor activity of gold(I), silver(I) and copper(I) complexes containing chiral tertiary phosphines. *Met. Based Drugs* **1998**, *5*, 217–223. [[CrossRef](#)]
15. Santini, C.; Pellei, M.; Papini, G.; Morresi, B.; Galassi, R.; Ricci, S.; Tisato, F.; Porchia, M.; Rigobello, M.P.; Gandin, V.; et al. In vitro antitumor activity of water soluble Cu(I), Ag(I) and Au(I) complexes supported by hydrophilic alkyl phosphine ligands. *J. Inorg. Biochem.* **2011**, *105*, 232–240. [[CrossRef](#)]
16. Berners-Price, S.J.; Bowen, R.J.; Galettis, P.; Healy, P.C.; McKeage, M.J. Structural and solution chemistry of gold(I) and silver(I) complexes of bidentate pyridyl phosphines: Selective antitumor agents. *Coord. Chem. Rev.* **1999**, *185–186*, 823–836. [[CrossRef](#)]
17. Papini, G.; Bandoli, G.; Dolmella, A.; Lobbia, G.G.; Pellei, M.; Santini, C. New homoleptic carbene transfer ligands and related coinage metal complexes. *Inorg. Chem. Commun.* **2008**, *11*, 1103–1106. [[CrossRef](#)]
18. Banti, C.N.; Hadjikakou, S.K. Anti-proliferative and anti-tumor activity of silver(i) compounds. *Metallomics* **2013**, *5*, 569–596. [[CrossRef](#)]
19. Shi, T.; Sun, X.; He, Q.Y. Cytotoxicity of silver nanoparticles against bacteria and tumor cells. *Curr. Protein Pept. Sci.* **2018**, *19*, 525. [[CrossRef](#)]
20. Jin, X.; Tan, X.; Zhang, X.; Han, M.; Zhao, Y. In vitro and in vivo anticancer effects of singly protonated dehydronorcantharidin silver coordination polymer in CT-26 murine colon carcinoma model. *Bioorg. Med. Chem. Lett.* **2015**, *25*, 4477. [[CrossRef](#)]
21. Chen, X.; Yang, Q.; Chen, J.; Zhang, P.; Huang, Q.; Zhang, X.; Yang, L.; Xu, D.; Zhao, C.; Wang, X.; et al. Inhibition of proteasomal deubiquitinase by silver complex induces apoptosis in non-small cell lung cancer cells. *Cell. Physiol. Biochem.* **2018**, *49*, 780. [[CrossRef](#)] [[PubMed](#)]
22. Medvetz, D.A.; Hindi, K.M.; Panzner, M.J.; Ditto, A.J.; Yun, Y.H.; Youngs, W.J. Anticancer activity of Ag(I) N-heterocyclic carbene complexes derived from 4,5-dichloro-1H-imidazole. *Met. Based Drugs* **2008**, *2008*, 384010. [[CrossRef](#)] [[PubMed](#)]
23. Marinelli, M.; Pellei, M.; Cimarelli, C.; Dias, H.V.R.; Marzano, C.; Tisato, F.; Porchia, M.; Gandin, V.; Santini, C. Novel multicharged silver(I)-NHC complexes derived from zwitterionic 1,3-symmetrically and 1,3-unsymmetrically substituted imidazoles and benzimidazoles: Synthesis and cytotoxic properties. *J. Organomet. Chem.* **2016**, *806*, 45–53. [[CrossRef](#)]
24. Pellei, M.; Gandin, V.; Marinelli, M.; Orsetti, A.; Del Bello, F.; Santini, C.; Marzano, C. Novel triazolium based 11th group NHCs: Synthesis, characterization and cellular response mechanisms. *Dalton Trans.* **2015**, *44*, 21041–21052. [[CrossRef](#)]
25. Wei, L.; Lu, J.; Xu, H.; Patel, A.; Chen, Z.S.; Chen, G. Silver nanoparticles: Synthesis, properties, and therapeutic applications. *Drug Discov. Today* **2015**, *20*, 595. [[CrossRef](#)]
26. Beck, A.; Weibert, B.; Burzlaff, N. Monoanionic N,N,O-scorpionate ligands and their iron(II) and zinc(II) complexes: Models for mononuclear active sites of non-heme iron oxidases and zinc enzymes. *Eur. J. Inorg. Chem.* **2001**, *2*, 521–527. [[CrossRef](#)]
27. Burzlaff, N.; Hegelmann, I.; Weibert, B. Bis(pyrazol-1-yl)acetates as tripodal “scorpionate” ligands in transition metal carbonyl chemistry: Syntheses, structures and reactivity of manganese and rhenium carbonyl complexes of the type [LM(CO)<sub>3</sub>] (L = bpza, bdmpta). *J. Organomet. Chem.* **2001**, *626*, 16–23. [[CrossRef](#)]

28. Otero, A.; Fernandez-Baeza, J.; Tejada, J.; Antinolo, A.; Carrillo-Hermosilla, F.; Diez-Barra, E.; Lara-Sanchez, A.; Fernandez-Lopez, M.; Lanfranchi, M.; Pellinghelli, M.A. Syntheses and crystal structures of lithium and niobium complexes containing a new type of monoanionic "scorpionate" ligand. *J. Chem. Soc. Dalton Trans.* **1999**, *20*, 3537–3539. [[CrossRef](#)]
29. Alkorta, I.; Claramunt, R.M.; Díez-Barra, E.; Elguero, J.; de la Hoz, A.; López, C. The organic chemistry of poly(1H-pyrazol-1-yl)methanes. *Coord. Chem. Rev.* **2017**, *339*, 153–182. [[CrossRef](#)]
30. Otero, A.; Fernández-Baeza, J.; Lara-Sánchez, A.; Sánchez-Barba, L.F. Metal complexes with heteroscorpionate ligands based on the bis(pyrazol-1-yl)methane moiety: Catalytic chemistry. *Coord. Chem. Rev.* **2013**, *257*, 1806–1868. [[CrossRef](#)]
31. Paul, T.; Rodehutsors, P.M.; Schmidt, J.; Burzlaff, N. Oxygen atom transfer catalysis with homogenous and polymer-supported N,N- and N,N,O-heteroscorpionate dioxidomolybdenum(VI) complexes. *Eur. J. Inorg. Chem.* **2016**, *2016*, 2595–2602. [[CrossRef](#)]
32. Fischer, N.V.; Türkoglu, G.; Burzlaff, N. Scorpionate complexes suitable for enzyme inhibitor studies. *Curr. Bioact. Compd.* **2009**, *5*, 277–295. [[CrossRef](#)]
33. Costas, M.; Mehn, M.P.; Jensen, M.P.; Que Jr, L. Dioxygen activation at mononuclear nonheme iron active sites: Enzymes, models, and intermediates. *Chem. Rev.* **2004**, *104*, 939–986. [[CrossRef](#)] [[PubMed](#)]
34. Parkin, G. Synthetic analogues relevant to the structure and function of zinc enzymes. *Chem. Rev.* **2004**, *104*, 699–767. [[CrossRef](#)] [[PubMed](#)]
35. Burzlaff, N. Tripodal N,N,O-ligands for metalloenzyme models and organometallics. In *Advances in Inorganic Chemistry*; van Eldik, R., Ed.; Elsevier: Amsterdam, The Netherlands, 2008; Volume 60, pp. 101–165.
36. Giorgetti, M.; Tonelli, S.; Zanelli, A.; Aquilanti, G.; Pellei, M.; Santini, C. Synchrotron radiation X-ray absorption spectroscopic studies in solution and electrochemistry of a nitroimidazole conjugated heteroscorpionate copper(II) complex. *Polyhedron* **2012**, *48*, 174–180. [[CrossRef](#)]
37. Pellei, M.; Papini, G.; Trasatti, A.; Giorgetti, M.; Tonelli, D.; Minicucci, M.; Marzano, C.; Gandin, V.; Aquilanti, G.; Dolmella, A.; et al. Nitroimidazole and glucosamine conjugated heteroscorpionate ligands and related copper(II) complexes. Syntheses, biological activity and XAS studies. *Dalton Trans.* **2011**, *40*, 9877–9888. [[CrossRef](#)] [[PubMed](#)]
38. Pellei, M.; Bagnarelli, L.; Luciani, L.; Del Bello, F.; Giorgioni, G.; Piergentili, A.; Quaglia, W.; De Franco, M.; Gandin, V.; Marzano, C.; et al. Synthesis and cytotoxic activity evaluation of new Cu(I) complexes of Bis(pyrazol-1-yl) acetate ligands functionalized with an NMDA receptor antagonist. *Int. J. Mol. Sci.* **2020**, *21*, 2616. [[CrossRef](#)]
39. Morelli, M.B.; Amantini, C.; Santoni, G.; Pellei, M.; Santini, C.; Cimarelli, C.; Marcantoni, E.; Petrini, M.; Del Bello, F.; Giorgioni, G.; et al. Novel antitumor copper(ii) complexes designed to act through synergistic mechanisms of action, due to the presence of an NMDA receptor ligand and copper in the same chemical entity. *New J. Chem.* **2018**, *42*, 11878–11887. [[CrossRef](#)]
40. Pellei, M.; Gandin, V.; Cimarelli, C.; Quaglia, W.; Mosca, N.; Bagnarelli, L.; Marzano, C.; Santini, C. Syntheses and biological studies of nitroimidazole conjugated heteroscorpionate ligands and related Cu(I) and Cu(II) complexes. *J. Inorg. Biochem.* **2018**, *187*, 33–40. [[CrossRef](#)]
41. Del Bello, F.; Pellei, M.; Bagnarelli, L.; Santini, C.; Giorgioni, G.; Piergentili, A.; Quaglia, W.; Battocchio, C.; Iucci, G.; Schiesaro, I.; et al. Cu(I) and Cu(II) complexes based on lonidamine-conjugated ligands designed to promote synergistic antitumor effects. *Inorg. Chem.* **2022**, *61*, 4919–4937. [[CrossRef](#)]
42. Pellei, M.; Santini, C.; Bagnarelli, L.; Battocchio, C.; Iucci, G.; Venditti, I.; Meneghini, C.; Amatori, S.; Sgarbossa, P.; Marzano, C.; et al. Exploring the antitumor potential of copper complexes based on ester derivatives of Bis(pyrazol-1-yl)acetate ligands. *Int. J. Mol. Sci.* **2022**, *23*, 9397. [[CrossRef](#)] [[PubMed](#)]
43. Gabrielli, S.; Pellei, M.; Venditti, I.; Fratoddi, I.; Battocchio, C.; Iucci, G.; Schiesaro, I.; Meneghini, C.; Palmieri, A.; Marcantoni, E.; et al. Development of new and efficient copper(II) complexes of hexyl bis(pyrazolyl)acetate ligands as catalysts for allylic oxidation. *Dalton Trans.* **2020**, *49*, 15622–15632. [[CrossRef](#)] [[PubMed](#)]
44. Bagnarelli, L.; Dolmella, A.; Santini, C.; Vallesi, R.; Giacomantonio, R.; Gabrielli, S.; Pellei, M. A new dimeric Copper(II) complex of hexyl bis(pyrazolyl)acetate ligand as an efficient catalyst for allylic oxidations. *Molecules* **2021**, *26*, 6271. [[CrossRef](#)] [[PubMed](#)]
45. Pellei, M.; Bagnarelli, L.; Gabrielli, S.; Lupidi, G.; Cimarelli, C.; Stella, F.; Dolmella, A.; Santini, C. Copper(II) complexes based on isopropyl ester derivatives of bis(pyrazol-1-yl)acetate ligands with catalytic potency in organic macro(molecules) synthesis. *Inorg. Chim. Acta* **2023**, *544*, 121234. [[CrossRef](#)]
46. Geary, W.J. The use of conductivity measurements in organic solvents for the characterisation of coordination compounds. *Coord. Chem. Rev.* **1971**, *7*, 81–122. [[CrossRef](#)]
47. Gill, D.S.; Rana, D. Preparation of some novel copper(I) complexes and their molar conductances in organic solvents. *Z. Naturforsch.* **2009**, *64*, 269–272. [[CrossRef](#)]
48. Effendy; Gioia Lobbia, G.; Marchetti, F.; Pellei, M.; Pettinari, C.; Pettinari, R.; Santini, C.; Skelton, B.W.; White, A.H. Syntheses and spectroscopic and structural characterization of silver(I) complexes containing tris(isobutyl)phosphine and poly(azol-1-yl)borates. *Inorg. Chim. Acta* **2004**, *357*, 4247–4256. [[CrossRef](#)]
49. Pellei, M.; Alidori, S.; Papini, G.; Lobbia, G.G.; Gorden, J.D.; Dias, H.V.R.; Santini, C. Silver(i)-organophosphane complexes of electron withdrawing CF<sub>3</sub>- or NO<sub>2</sub>-substituted scorpionate ligands. *Dalton Trans.* **2007**, *42*, 4845–4853. [[CrossRef](#)]
50. Dias, H.V.R.; Flores, J.A.; Pellei, M.; Morresi, B.; Lobbia, G.G.; Singh, S.; Kobayashi, Y.; Yousufuddin, M.; Santini, C. Silver(I) and copper(I) complexes supported by fully fluorinated 1,3,5-triazapentadienyl ligands. *Dalton Trans.* **2011**, *40*, 8569–8580. [[CrossRef](#)]



51. Marverti, G.; Andrews, P.A.; Piccinini, G.; Ghiaroni, S.; Barbieri, D.; Moruzzi, M.S. Modulation of cis-diamminedichloroplatinum (II) accumulation and cytotoxicity by spermine in sensitive and resistant human ovarian carcinoma cells. *Eur. J. Cancer* **1997**, *33*, 669–675. [[CrossRef](#)]
52. Andrews, P.A.; Murphy, M.P.; Howell, S.B. Differential potentiation of alkylating and platinating agent cytotoxicity in human ovarian carcinoma cells by glutathione depletion. *Cancer Res.* **1985**, *45*, 6250–6253. [[PubMed](#)]
53. Scanlon, K.J.; Kashani-Sabet, M.; Tone, T.; Funato, T. Cisplatin resistance in human cancers. *Pharmacol. Ther.* **1991**, *52*, 385–406. [[CrossRef](#)] [[PubMed](#)]
54. Marzano, C.; Gandin, V.; Folda, A.; Scutari, G.; Bindoli, A.; Rigobello, M.P. Inhibition of thioredoxin reductase by auranofin induces apoptosis in cisplatin-resistant human ovarian cancer cells. *Free Radic. Biol. Med.* **2007**, *42*, 872–881. [[CrossRef](#)]
55. Kunz-Schughart, L.A.; Freyer, J.P.; Hofstaedter, F.; Ebner, R. The use of 3-D cultures for high-throughput screening: The multicellular spheroid model. *J. Biomol. Screen.* **2004**, *9*, 273–285. [[CrossRef](#)] [[PubMed](#)]
56. Gandin, V.; Fernandes, A.P. Metal- and semimetal-containing inhibitors of thioredoxin reductase as anticancer agents. *Molecules* **2015**, *20*, 12732–12756. [[CrossRef](#)] [[PubMed](#)]
57. De Franco, M.; Saab, M.; Porchia, M.; Marzano, C.; Nolan, S.P.; Nahra, F.; Van Hecke, K.; Gandin, V. Unveiling the potential of innovative gold(I) and silver(I) selenourea complexes as anticancer agents targeting TrxR and cellular redox homeostasis. *Chem. Eur. J.* **2022**, *28*, e202201898. [[CrossRef](#)] [[PubMed](#)]
58. Cheng, Y.; Qi, Y. Current progresses in metal-based anticancer complexes as mammalian TrxR inhibitors. *Anti-Cancer Agents Med. Chem.* **2017**, *17*, 1046–1069. [[CrossRef](#)]
59. Björkhem-Bergman, L.; Jönsson-Videsäter, K.; Paul, C.; Björnstedt, M.; Andersson, M. Mammalian thioredoxin reductase alters cytolytic activity of an antibacterial peptide. *Peptides* **2004**, *25*, 1849–1855. [[CrossRef](#)]
60. Bebbler, C.M.; von Karstedt, S. Non-neuroendocrine differentiation generates a ferroptosis-prone lipidome in small cell lung cancer (SCLC). *Mol. Cell. Oncol.* **2021**, *8*, 1933871. [[CrossRef](#)]
61. Galassi, R.; Burini, A.; Ricci, S.; Pellei, M.; Rigobello, M.P.; Citta, A.; Dolmella, A.; Gandin, V.; Marzano, C. Synthesis and characterization of azolate gold(i) phosphane complexes as thioredoxin reductase inhibiting antitumor agents. *Dalton Trans.* **2012**, *41*, 5307–5318. [[CrossRef](#)]
62. Arnér, E.S.J. Focus on mammalian thioredoxin reductases—Important selenoproteins with versatile functions. *Biochim. Biophys. Acta. Gen. Subj.* **2009**, *1790*, 495–526. [[CrossRef](#)] [[PubMed](#)]
63. Scalcon, V.; Bindoli, A.; Rigobello, M.P. Significance of the mitochondrial thioredoxin reductase in cancer cells: An update on role, targets and inhibitors. *Free Radic. Biol. Med.* **2018**, *127*, 62–79. [[CrossRef](#)] [[PubMed](#)]
64. Suski, J.; Lebiecinska, M.; Bonora, M.; Pinton, P.; Duszynski, J.; Wieckowski, M.R. Relation between mitochondrial membrane potential and ROS formation. In *Mitochondrial Bioenergetics: Methods and Protocols*; Palmeira, C.M., Moreno, A.J., Eds.; Springer: New York, NY, USA, 2018; pp. 357–381.
65. Porchia, M.; Papini, G.; Santini, C.; Lobbia, G.G.; Pellei, M.; Tisato, F.; Bandoll, G.; Dolmella, A. Novel rhenium(V) oxo complexes containing bis(pyrazol-1-yl)acetate and bis(pyrazol-1-yl) sulfonate as tripodal N,N,O-heteroscorpionate ligands. *Inorg. Chem.* **2005**, *44*, 4045–4054. [[CrossRef](#)] [[PubMed](#)]
66. Hübner, E.; Haas, T.; Burzlaff, N. Synthesis and transition metal complexes of novel N,N,O scorpionate ligands suitable for solid phase immobilisation. *Eur. J. Inorg. Chem.* **2006**, *24*, 4989–4997. [[CrossRef](#)]
67. Zheng, Z.; Groaz, E.; Snoeck, R.; De Jonghe, S.; Herdewijn, P.; Andrei, G. Influence of 4'-substitution on the activity of gemcitabine and its ProTide against VZV and SARS-CoV-2. *ACS Med. Chem. Lett.* **2020**, *12*, 88–92. [[CrossRef](#)] [[PubMed](#)]
68. Rigobello, M.P.; Gandin, V.; Folda, A.; Rundlöf, A.-K.; Fernandes, A.P.; Bindoli, A.; Marzano, C.; Björnstedt, M. Treatment of human cancer cells with selenite or tellurite in combination with auranofin enhances cell death due to redox shift. *Free Radic. Biol. Med.* **2009**, *47*, 710–721. [[CrossRef](#)]

**Disclaimer/Publisher's Note:** The statements, opinions and data contained in all publications are solely those of the individual author(s) and contributor(s) and not of MDPI and/or the editor(s). MDPI and/or the editor(s) disclaim responsibility for any injury to people or property resulting from any ideas, methods, instructions or products referred to in the content.